SNR Analysis of the Millimeter Wave MIMO with Lens Antenna Array

Min Zhang[1(✉)], Jianxin Dai[2], Chonghu Cheng[1], and Zhiliang Huang[3]

[1] College of Telecommunications & Information Engineering, Nanjing University of Posts and Telecommunications, Nanjing 210003, China
2810729610@qq.com, chengch@njupt.edu.cn
[2] School of Science, Nanjing University of Posts and Telecommunications, Nanjing 210023, China
daijx@njupt.edu.cn
[3] College of Mathematics, Physics and Information Engineering, Zhejiang Normal University, Jinhua 321004, China
zlhuang@zjnu.cn

Abstract. The lens antenna array is typically composed of an electromagnetic (EM) lens and has elements in the focal area of the lens in order to achieve its large antenna gain. In this paper, we first analyze the response model of the lens antenna array, and conclude that the model follows the "sinc" function. The lens array is then applied to a MIMO system that allows millimeter-wave input and the use of new path-division multiplexing. On this basis, we model the channel of the system to derive the channel impulse response, which follows the "sinc sinc" function. Finally, the beamforming process is performed at the receiving end to obtain the received signal, and the signal-to-noise ratio expression is analyzed and optimized to obtain the maximum signal-to-noise ratio (SNR) of the system and the system performance is simulated.

Keywords: Millimeter wave · Lens antenna array · Signal-to-noise ratio
Path-division multiplexing · AoA/AoD

1 Introduction

According to the development law of mobile communication, 5G will be better than 4G mobile communication in terms of transmission rate and resource utilization. Nowadays, 5G has become a research hotspot in the field of mobile communication at home and abroad.

(1) On May 29, 2015, Coolpad first mentioned 5G new concept: terminal base station.
(2) On June 24, 2015, the International Telecommunication Union (ITU) announced a timetable for the 5G technical standardization. The official name of the 5G technology is IMT-2020 and the 5G standard will be finalized by 2020.
(3) On January 7, 2016, the Ministry of Industry held a meeting announcing the "5G technology research and development test".

X. Gu et al. (Eds.): MLICOM 2017, Part I, LNICST 226, pp. 505–515, 2018.
https://doi.org/10.1007/978-3-319-73564-1_50

(4) On February 9, 2017, the international communications standards organization 3GPP announced the "5G" official Logo.

However, the low frequency of the radio spectrum has become saturated because of the rapid development of communication industry, so the future development needs can not be met, which leads people to seek higher spectrum. Millimeter wave has the characteristics of short wavelength and wide frequency band, having the ability to solve many problems faced by future development of communication. Also it has a wide range of applications in short distance communication. For traditional communication systems, Multiple Input Multiple Output (MIMO) technology can increase the spectrum utilization to a great extent, making the system transmit higher-speed data services in a limited wireless band. With the development of technology, the future of 5G communication broadband or wireless access integration system has become a popular research topic, and MIMO system is one of the more people to study the direction [1–5]. The MmWave signal typically suffers from more path losses than frequencies that are much lower at a given distance at an existing cellular system. So efficient MIMO technology can be used to compensate for severe path losses, which achieves highly directional communication [6–9]. The general MIMO processing is usually digitally realized at the baseband, so a special radio frequency (RF) chain is set for communication. However, in the mmWave system, we generally do not take this approach because a large number of RF chain hardware costs are relatively large. In order to realize spatial reuse, hybrid analog/digital precoding has been proposed, in which precoding is implemented in two phases. Due to the need of many phase shifters in the case of hybrid precoding, it is also proposed to select the subset of antennas by using the switch instead of the phase shifter. However, because of the limited array gain, antenna selection can lead to significant performance degradation [10–14]. In our study, the mmWave MIMO communications is analyzed, where a lens antenna array is applied in the transmitter and receiver. Because of the energy focusing characteristics of AoA/AoD, the signal power in the mmWave lens MIMO with a limited number of multipath is usually concentrated only on the small set of the receiver/transmitter antenna elements.

The following structure of the article is described below: the system model is introduced in the second section. The third section mainly analyzes the SNR ratio. The fourth section shows the numerical simulation results. The fifth section is the summary of the full paper.

2 System Model

2.1 Analysis of Lens Antenna Array

In optics, the spherical wave radiated by a point light source placed on the focal point of a lens is refracted into a plane wave by refraction of a lens. The lens antenna is made by this principle. Figure 1 shows the configuration of the lens antenna array. It is easy to see that the array element happens to be located in the focal region of the lens. In generally, EM lens can be realized through some techniques,such as a conventional planar lens composed of transmit and receive antenna arrays with variable length

transmission lines. No matter what the actual realization, the fundamental of the EM lens is to offer a variable phase shift to the EM rays of the lens, with the aim of achieving the energy focusing properties depending on the angle. In particular, the receiving lens antenna array can be used to focus the incident signal to a plurality of receiving antenna subsets with sufficient separation angle of arrival (AoA). Similarly, the emission lens array can be used to manipulate the deviation signal from a subset of different transmit antennas with a sufficient separation of the angle of departure (AoD) [15].

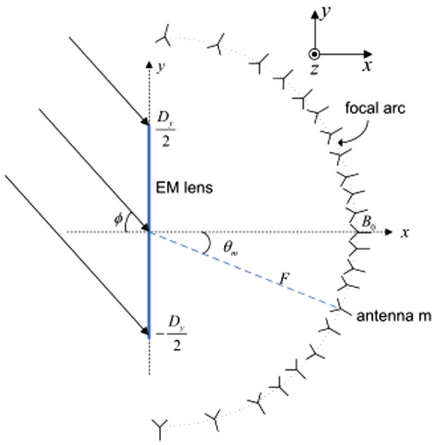

Fig. 1. An example of a lens receiving a plane wave incident.

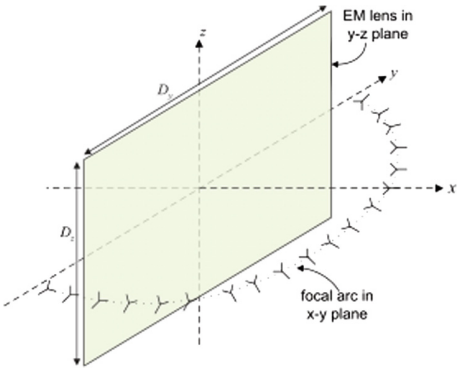

Fig. 2. A stereogram of a lens antenna array.

In this paper, we placed a plane EM lens on the yz plane, making it centered on the origin. Its size is Dy $\times$ Dz, which can be neglected, as exhibited in Fig. 2. Only taking the azimuth angles AoA and AoD into consideration, in Fig. 1, it is assumed that the

array element is set on a semicircle around the center of a lens in a plane. The semicircle has a radius of F, which is called the focal length of the lens. Thus, the antenna position of the lens antenna array can be mathematically expressed as $B_m \quad (x_m = F\cos\theta_m, y_m = -F\sin\theta_m, z_m = 0)$, where $\theta_m \in [-\pi/2, \pi/2]$ is the m-th antenna element's angle with respect to the x-axis, $m \in M$, and M represents the total number of antennas using in the lens antenna array. For convenience, we assume that M is odd. In addition, we assume that the antenna has a critical antenna spacing, for example, the antenna element is deployed on the coke arc, making $\{\tilde{\theta}_m \triangleq \sin\theta_m\}$ in the interval [−1,1] equally spaced, i.e. $\tilde{\theta}_m = \frac{m}{D}, m \in M$, where $\tilde{D} = \frac{D_y}{\lambda}$ is the size of the lens in antenna array and normalized by the carrier wavelength λ. Besides, M and $\tilde{D}$ are satisfied $M = 1 + \lfloor 2\tilde{D} \rfloor$, i.e., for larger lens sizes $\tilde{D}$, more antennas should be deployed. Naturally, with the specified deployment of the antenna array, the number of antennas at the two edges of the array is less than that in the center.

First of all, let us assume that the lens antenna array is irradiated with a uniform plane wave with AoA ϕ to study the reception array response, as shown in Fig. 1. $x_o(\phi)$ represents an incident signal whose point of incidence is located on the reference point on the lens (for example, the center of the lens), and $r_m(\phi)$ represents the receiving signal by the m-th element [15], $m \in M$. In addition, the response vector of the array is $\boldsymbol{a}(\phi) \in C^{M\times 1}$, whose element $a_m(\phi) = \frac{r_m(\phi)}{x_o(\phi)}$ can be shown as

$$a_m(\phi) \approx e^{-j\phi_o}\sqrt{A}\,\sin c(m - \tilde{D}\tilde{\phi}), m \in M \tag{1}$$

where ϕ is the angle of arrival (AoA), $A \triangleq D_y D_z/\lambda^2$ is the normalized aperture, i.e., the physical area of the EM lens normalized by wavelength squares, ϕ_0 is the common phase shift from the lens aperture to the array [15], and $\tilde{\phi} \triangleq \sin\phi \in [-1, 1]$ is called the spatial frequency corresponding to AoA ϕ.

Without loss of generality, for an integer n in the remainder of the text, we have $\phi_o = 2n\pi$, making it possible to ignore the phase term in (1), thus the expression (1) becomes

$$a_m(\phi) = \sqrt{A}\,\sin c(m - \tilde{D}\tilde{\phi}), m \in M \tag{2}$$

As we all know, the incident and outgoing signals passing through the EM lens remain interchangeable because the EM lenses are passive devices. Therefore, the transmission response vector that turns the signal to AoD ϕ can be obtained in the same way. The details are omitted for simplicity.

2.2 Analysis of Channel Model

In this section, a special MIMO transceiver that based on Path Division Multiplexing (PDM) is designed, which is suitable for narrowband and broadband mmWave communication. Using PDM, L independent data streams are typically transmitted via transmit beamforming/precoding, each of which passes through one of the

L multi-paths. In particular, the discrete time equivalent of the transmitted signal $\boldsymbol{x}_{Qs}[t]$ may be expressed as

$$\boldsymbol{x}_{Qs}[n] = \sum_{l=1}^{L} \sqrt{\frac{p_l}{A_T}} \boldsymbol{a}_{T,Qs}(\phi_{T,l}) s_l[n] \tag{3}$$

where n represents the symbol index, $s_l[n] \sim CN(0,1)$ (circle symmetric complex Gaussian) represents the independent CSCG distributed information bearing symbol with the transmit power p_l for the data stream; and $\boldsymbol{a}_{T,Qs}(\phi_{T,l})/A_T$ represents the unit norm of the AoD $\phi_{T,l}$ towards path l per path MRT beamforming vector. Note that we use $\left\|\boldsymbol{a}_{T,Qs}(\phi_{T,l})\right\|^2 \approx \left\|\boldsymbol{a}_T(\phi_{T,l})\right\|^2 = A_T, \forall l$. At the receiving end, we apply a low complexity detection to the receive signal, where the beamforming vector $\boldsymbol{v}_l \in C^{M_S \times 1}$ is received and $\|\boldsymbol{v}_l\| = 1$.

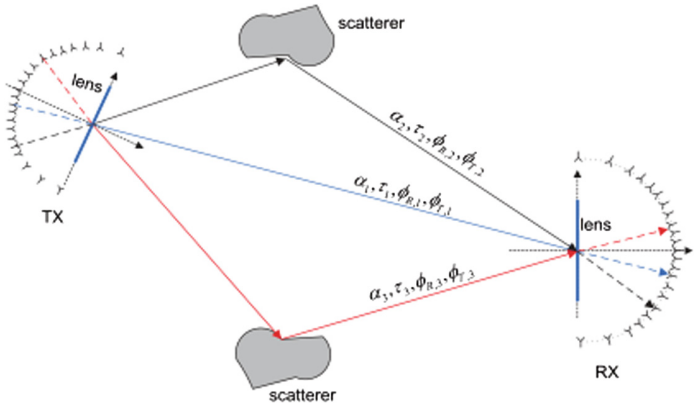

Fig. 3. The schematic diagram of multi-path environment.

As shown in the Fig. 3, at the transmitter and receiver, we set Q and M antenna elements. In a typical MIMO system, the channel impulse response can be represented as

$$\boldsymbol{H}(t) = \sum_{l=1}^{L} \alpha_l \boldsymbol{a}_R(\phi_{R,l}) \boldsymbol{a}_T^H(\phi_{T,l}) \delta(t - \tau_l) \tag{4}$$

The signal at the receiving end is

$$\boldsymbol{r}(t) = \boldsymbol{H}(t) * \boldsymbol{x}(t) + \boldsymbol{z}(t) \tag{5}$$

$$\boldsymbol{r}(t) = \sum_{l=1}^{L} \alpha_l \boldsymbol{a}_R(\phi_{R,l}) \boldsymbol{a}_T^H(\phi_{T,l}) \boldsymbol{x}(t - \tau_l) + \boldsymbol{z}(t) \tag{6}$$

However, because there is multipath sparsity in mmWave communication, the discrete received signal at the receiving end in this system is expressed as

$$\boldsymbol{r}_{Ms}[n] = \sum_{k=1}^{L} \alpha_k \boldsymbol{a}_{R,k} \boldsymbol{a}_{T,k}^H \boldsymbol{x}_{Qs}[n - n_k] + \boldsymbol{z}_{Ms}[n] \tag{7}$$

where each component is a subset of the components in the expression (6).

We decompose the received signal in the expression (7) into the desired signal passing through the l-th path, which has the symbol delay nl; the ISI from the other $L - 1$ paths, which have different delays; and the other $L - 1$ data streams interference from the L signal paths, which are as the expression (8) [15].

$$\begin{aligned} r_{Ms}[n] = {} & \sqrt{p_l A_T} \alpha_l \boldsymbol{a}_{R,l} s_l[n - n_l] + \sum_{k \neq l}^{L} \sqrt{\frac{p_l}{A_T}} \alpha_k \boldsymbol{a}_{R,k} \boldsymbol{a}_{T,k}^H \boldsymbol{a}_{T,l} s_l[n - n_k] \\ & + \sum_{l' \neq l}^{L} \sum_{k=1}^{L} \sqrt{\frac{p_{l'}}{A_T}} \alpha_k \boldsymbol{a}_{R,k} \boldsymbol{a}_{T,k}^H \boldsymbol{a}_{T,l'} s_{l'}[n - n_k] + z_{Ms}[n] \end{aligned} \tag{8}$$

The receiver beamforming is applied in the above equation [20, 21], besides, ISI together with inter-stream interference are treated as interference [16–18]. Thus the effective SNR of the l-th data stream at the receiver is shown as

$$\gamma_l = \frac{p_l A_T |\alpha_l|^2 \left| \boldsymbol{v}_l^H \boldsymbol{a}_{R,l} \right|^2}{\sum_{k \neq l}^{L} \frac{p_l}{A_T} |\alpha_k|^2 \left| \boldsymbol{v}_l^H \boldsymbol{a}_{R,k} \right|^2 \left| \boldsymbol{a}_{T,k}^H \boldsymbol{a}_{T,l} \right|^2 + \sum_{l' \neq l}^{L} \sum_{k=1}^{L} \frac{p_{l'}}{A_T} |\alpha_k|^2 \left| \boldsymbol{v}_l^H \boldsymbol{a}_{R,k} \right|^2 \left| \boldsymbol{a}_{T,k}^H \boldsymbol{a}_{T,l'} \right|^2 + \boldsymbol{v}_l^H \sigma^2 \boldsymbol{v}_l} \tag{9}$$

3 Analysis and Optimization

SNR is a measure of communication system communication quality reliability of a major technical indicator. The SNR is generally the ratio of the channel output, that is, the average power of the carrier signal at the receiver input to that of the noise in the channel. It can also be called a carrier to noise ratio. Increasing or improving signal-to-noise ratio is a major task in improving communication quality. In the following, we will optimize the SNR expression in (9) to obtain the maximum signal-to-noise ratio of the millimeter wave MIMO system.

The part of the beamforming vector is split into

$$\gamma_l = \frac{p_l A_T |\alpha_l|^2 \boldsymbol{v}_l^H \boldsymbol{a}_{R,l} \boldsymbol{a}_{R,l}^H \boldsymbol{v}_l}{\sum_{k \neq l}^{L} \frac{p_l}{A_T} |\alpha_k|^2 \boldsymbol{v}_l^H \boldsymbol{a}_{R,k} \boldsymbol{a}_{R,k}^H \boldsymbol{v}_l \left| \boldsymbol{a}_{T,k}^H \boldsymbol{a}_{T,l} \right|^2 + \sum_{l' \neq l}^{L} \sum_{k=1}^{L} \frac{p_{l'}}{A_T} |\alpha_k|^2 \boldsymbol{v}_l^H \boldsymbol{a}_{R,k} \boldsymbol{a}_{R,k}^H \boldsymbol{v}_l \left| \boldsymbol{a}_{T,k}^H \boldsymbol{a}_{T,l'} \right|^2 + \boldsymbol{v}_l^H \sigma^2 \boldsymbol{v}_l} \tag{10}$$

Extracting the beamforming vector, then we get

$$\gamma_l = \frac{\boldsymbol{v}_l^H p_l A_T |\alpha_l|^2 \boldsymbol{a}_{R,l} \boldsymbol{a}_{R,l}^H \boldsymbol{v}_l}{\boldsymbol{v}_l^H \left(\sum_{k \neq l}^{L} \frac{p_l}{A_T} |\alpha_k|^2 \boldsymbol{a}_{R,k} \boldsymbol{a}_{R,k}^H \left| \boldsymbol{a}_{T,k}^H \boldsymbol{a}_{T,l} \right|^2 + \sum_{l' \neq l}^{L} \sum_{k=1}^{L} \frac{p_{l'}}{A_T} |\alpha_k|^2 \boldsymbol{a}_{R,k} \boldsymbol{a}_{R,k}^H \left| \boldsymbol{a}_{T,k}^H \boldsymbol{a}_{T,l'} \right|^2 + \sigma^2 \boldsymbol{I} \right) \boldsymbol{v}_l} \tag{11}$$

Let $A = p_l A_T |\alpha_l|^2 \boldsymbol{a}_{R,l} \boldsymbol{a}_{R,l}^H$, which is a $Ms \times Ms$ order matrix; $B = \sum_{k \neq l}^{L} \frac{p_l}{A_T} |\alpha_k|^2 \boldsymbol{a}_{R,k} \boldsymbol{a}_{R,k}^H \left| \boldsymbol{a}_{T,k}^H \boldsymbol{a}_{T,l} \right|^2 + \sum_{l' \neq l}^{L} \sum_{k=1}^{L} \frac{p_{l'}}{A_T} |\alpha_k|^2 \boldsymbol{a}_{R,k} \boldsymbol{a}_{R,k}^H \left| \boldsymbol{a}_{T,k}^H \boldsymbol{a}_{T,l'} \right|^2 + \sigma^2 \boldsymbol{I}$, which is a $Ms \times Ms$ order matrix.

Then,

$$\gamma_l = \frac{\boldsymbol{v}_l^H A \boldsymbol{v}_l}{\boldsymbol{v}_l^H B \boldsymbol{v}_l} \tag{12}$$

Derive the expression (12)

$$\gamma_l' = \frac{A \boldsymbol{v}_l \boldsymbol{v}_l^H B \boldsymbol{v}_l - B \boldsymbol{v}_l \boldsymbol{v}_l^H A \boldsymbol{v}_l}{\left(\boldsymbol{v}_l^H B \boldsymbol{v}_l \right)^2} \tag{13}$$

Let the expression (13) be equal to 0,

$$A \boldsymbol{v}_l \boldsymbol{v}_l^H B \boldsymbol{v}_l = B \boldsymbol{v}_l \boldsymbol{v}_l^H A \boldsymbol{v}_l \tag{14}$$

Rearranging the equation, we get

$$A \boldsymbol{v}_l = \frac{\boldsymbol{v}_l^H A \boldsymbol{v}_l}{\boldsymbol{v}_l^H B \boldsymbol{v}_l} B \boldsymbol{v}_l \tag{15}$$

Therefore,

$$A \boldsymbol{v}_l = \gamma_l B \boldsymbol{v}_l \tag{16}$$

$$B^{-1} A \boldsymbol{v}_l = \gamma_l \boldsymbol{v}_l \tag{17}$$

Hence, the maximum value of the SNR ratio γ_l is the maximum eigenvalue of $B^{-1}A$, and the beamforming vector at this time is the eigenvector corresponding to the largest eigenvalue of $B^{-1}A$ [19–21].

4 Simulation and Results

In this section, MATLAB is utilized to simulate the performance of a MIMO system which uses the proposed lens antenna array and allows millimeter-wave input. It is assumed that the lens apertures are AT = 100 and AR = 50 respectively at the

transmitter and receiver. The input mmWave frequency is 73 GHz. And also azimuthal lens sizes at the transmitter and receiver are $\tilde{D}_T = 20$ and $\tilde{D}_R = 10$ respectively. For simplicity, here we assume all path power pl (l = 1, … L) is evenly distributed.

The maximum signal-to-noise ratio of the system has been given in the paper. Here we give different system configurations. And the performance of the system is simulated and compared based on these configurations. The comparison of system performance under these different configurations will help us to further study the millimeter-wave MIMO communication.

Figure 4 shows the variation of the maximum SNR ratio versus the multipath number in different number of antenna configurations at the receiving and transmitting ends. Here are three cases where the number of antennas at the transmitting and receiving ends is 31 and 51, 21 and 41 respectively, and both are 41. Obviously, with the increase of the number of multipaths, the maximum SNR ratio at the receiver decreases, that is, the performance of the system decreases and the trend slows down. In the case of a certain number of multipaths, when the number of antennas at the transmitting end is larger than that of antennas on the receiving side, the system performance is the best. As can be seen from the Fig. 4, when the number of transmit antennas and antennas on the receiving side are 41 and 21, the maximum SNR ratio is greater than the other two configurations. While the system performance is the worst when the number of transmit antennas is less than that of antennas on the receiving side. The maximum SNR ratio is smaller when the number of antennas on the receiving side are 31 and 51, as is shown in Fig. 4.

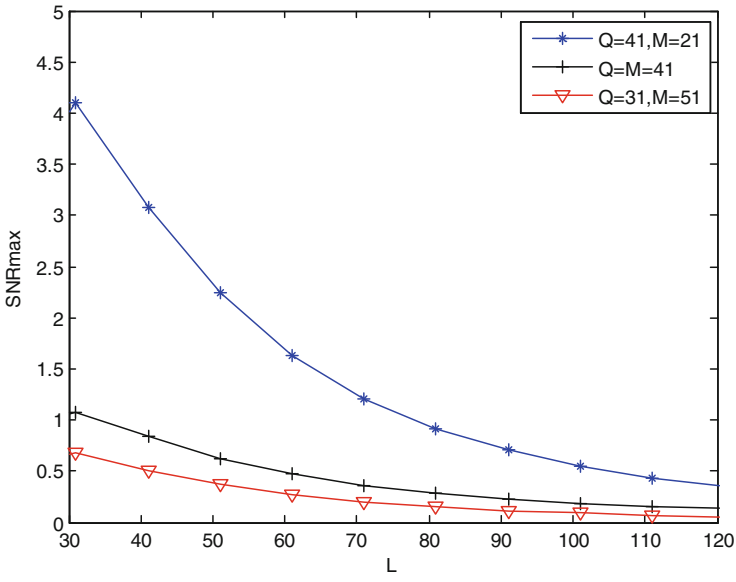

Fig. 4. The maximum signal-to-noise ratio versus the number of multipath under different numbers of antennas at the receiver and transmitter.

Figure 5 depicts curve of the maximum SNR versus the number of multipath at different spatial frequencies. When the multipath number is the same, the larger the spatial frequency interval of the antenna, the better the performance of the system. It can be seen that the curve of the maximum signal-to-noise ratio is more and more upward when the spatial interval changes from [−0.25, 0.25], [−0.5, 0.5] to [−0.7, 0.7]. And the maximum SNR ratio of the system with the spatial interval [−0.7, 0.7] is the largest when the multipath number L is fixed.

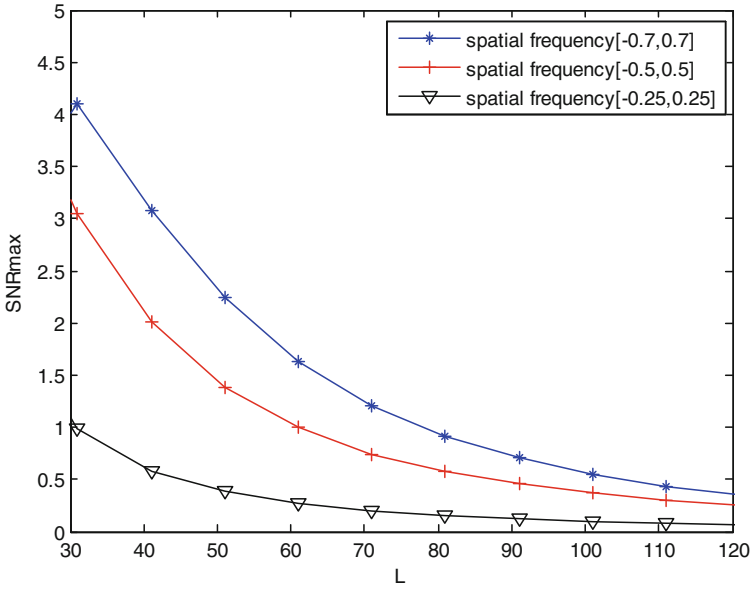

Fig. 5. The maximum signal-to-noise ratio versus the number of multipath at different spatial frequencies.

5 Conclusion

As the key technology of 5G, millimeter wave has become one of the hotspots of current research. In this paper, a millimeter-wave MIMO system model based on lens array is established, and a new path segmentation technique is used to analyze the SNR of the system. In communication systems, the signal power often needs to be increased as much as possible while suppressing noise and various disturbances within the system. The maximum SNR expression of millimeter-wave MIMO system is deduced theoretically in this paper. Based on the maximum SNR expression, the performance of a lens MIMO system with mmWave input is evaluated by simulation and we can easily find with the increase in the number of multipath, the maximum SNR is gradually reduced. Besides, the maximum SNR is important for us to study the performance of millimeter-wave MIMO systems and to lay the foundation for further research.

Acknowledgments. The research was supported in part by Postdoctoral Research Funding Plan in Jiangsu Province (Grant No. 1501073B), Natural Science Foundation of Nanjing University of Posts and Telecommunications (Grant No. NY214108), Natural Science Foundation of China (NSFC) (Grant No. 61401399), and the Open Research Fund of National Mobile Communications Research Laboratory, Southeast University (Grant No. 2016D05).

References

1. Ma, J., Li, H., Zhang, S., Zhao, N., Nallanathan, A.: Pattern division for massive MIMO networks with two-stage precoding. IEEE Commun. Lett. **21**(7), 1665–1668 (2017)
2. Xie, H., Gao, F., Zhang, S., Jin, S.: A unified transmission strategy for TDD/FDD massive MIMO systems with spatial basis expansion model. IEEE Trans. Veh. Technol. **66**(4), 3170–3184 (2017)
3. Xie, H., Gao, F., Jin, S.: An overview of low-rank channel estimation for massive MIMO systems. IEEE Access **4**, 7313–7321 (2016)
4. Xie, H., Wang, B., Gao, F., Jin, S.: A full-space spectrum-sharing strategy for massive MIMO cognitive radio. IEEE J. Sel. Areas Commun. **34**(10), 2537–2549 (2016)
5. Wang, J.-B., Chen, M., Wan, X., Wei, J.: Ant-colony-optimization-based scheduling algorithm for uplink CDMA nonreal-time data. IEEE Trans. Veh. Technol. **58**(1), 231–241 (2009)
6. Agrawal, S.K., Sharma, K.: 5G millimeter wave (mmWave) communications. In: 2016 3rd International Conference on Computing for Sustainable Global Development (INDIACom), New Delhi, pp. 3630–3634 (2016)
7. Zhang, J., Ge, X., Li, Q., Guizani, M., Zhang, Y.: 5G millimeter-wave antenna array: design and challenges. IEEE Wirel. Commun. **PP**(99), 2–8
8. Luo, F.-L., Zhang, C.: 5G millimeter-wave communication channel and technology overview. In: Signal Processing for 5G: Algorithms and Implementations, vol. 1, p. 616. Wiley-IEEE Press (2016)
9. Rangan, S., Rappaport, T.S., Erkip, E.: Millimeter-wave cellular wireless networks: potentials and challenges. Proc. IEEE **102**(3), 366–385 (2014)
10. Jing, J., Xiaoxue, C., Yongbin, X.: Energy-efficiency based downlink multi-user hybrid beamforming for millimeter wave massive MIMO system. J. China Univ. Posts Telecommun. **23**(4), 53–62 (2016)
11. Wang, J.-B., Qing-Song, H., Wang, J., Chen, M., Wang, J.-Y.: Tight bounds on channel capacity for dimmable visible light communications. IEEE/OSA J. Lightwave Technol. **31**(23), 3771–3779 (2013)
12. Wang, J.-Y., Wang, J.-B., Chen, M., Tang, Y., Zhang, Y.: Outage analysis for relay-aided free-space optical communications over turbulence channels with nonzero boresight pointing errors. IEEE Photonics J. **6**(4), 1–15 (2014)
13. Samimi, M.K., Sun, S., Rappaport, T.S.: MIMO channel modeling and capacity analysis for 5G millimeter-wave wireless systems. In: 2016 10th European Conference on Antennas and Propagation (EuCAP), Davos, pp. 1–5 (2016)
14. Rappaport, T.S., MacCartney, G.R., Samimi, M.K., Sun, S.: Wideband millimeter-wave propagation measurements and channel models for future wireless communication system design. IEEE Trans. Commun. **63**(9), 3029–3056 (2015)
15. Zeng, Y., Zhang, R.: Millimeter wave MIMO with lens antenna array: a new path division multiplexing paradigm. IEEE Trans. Commun. **64**(4), 1557–1571 (2016)

16. Liu, L., Matolak, D.W., Tao, C., Li, Y., Ai, B., Chen, H.: Channel capacity investigation of a linear massive MIMO system using spherical wave model in LOS scenarios. Sci. China Inf. Sci. **59**(2), 45–59 (2016)
17. Jin-Yuan, W., Jun-Bo, W., Nuo, H., Ming, C.: Capacity analysis for pulse amplitude modulated visible light communications with dimming control. J. Opt. Soc. Am. A **31**(3), 561–568 (2014)
18. Ali, S., Aslam, M.I., Ahmed, I.: MIMO channel modeling and capacity analysis using 3-D spatial statistical channel model for millimeter wave outdoor communication. In: 2017 14th International Bhurban Conference on Applied Sciences and Technology (IBCAST), Islamabad, pp. 735–740 (2017)
19. Samimi, M.K., Sun, S., Rappaport, T.S.: MIMO channel modeling and capacity analysis for 5G millimeter-wave wireless systems. In: 2016 10th European Conference on Antennas and Propagation (EuCAP), Davos, pp. 1–5 (2016)
20. Kamga, G.N., Xia, M., Aissa, S.: Channel modeling and capacity analysis of large MIMO in real propagation environments. In: 2015 IEEE International Conference on Communications (ICC), London, pp. 1447–1452 (2015)
21. Wang, J.-B., Su, Q., Wang, J., Feng, M., Chen, M., Jiang, B., Wang, J.-Y.: Imperfect CSI based joint resource allocation in multirelay OFDMA networks. IEEE Trans. Veh. Technol. **63**(8), 3806–3817 (2014)
22. Zhao, N., Yu, F.R., Leung, V.C.M.: Opportunistic communications in interference alignment networks with wireless power transfer. IEEE Wirel. Commun. **22**(1), 88–95 (2015)